APPLIED PHYSICS LETTERS VOLUME 85, NUMBER 22 29 NOVEMBER 2004

High-power 1.3-μm InGaAsN strain-compensated lasers fabricated with pulsed anodic oxidation

Yi Qu,[a] C. Y. Liu, and Shu Yuan[b]
School of Materials Engineering, Nanyang Technological University, Singapore 639798, Singapore

(Received 6 January 2004; accepted 14 October 2004)

Ridge waveguide InGaAsN triple-quantum-well strain-compensated lasers grown by metal-organic chemical vapor deposition were fabricated with pulsed anodic oxidation. Laser output power reached 962 mW in cw mode at room temperature from 100-μm stripe lasers with a wavelength of 1297 nm. The threshold-current density was 256 A/cm^2. The characteristic temperature of the lasers was 138 K in the linear region (20–80 °C).
[DOI: 10.1063/1.1828596]

Semiconductor lasers at wavelengths around 1.3 μm are widely used for fiber optic communications. It has been reported that the incorporation of nitrogen in InGaAs can reduce the band-gap energy and allows emission wavelengths as long as 1.3 μm to be reached.[1–10] However, high-performance 1.3-μm InGaAsN quantum-well (QW) lasers exhibit low characteristic temperature coefficients of threshold-current density, with only a slight improvement in T_0 values over those achieved by the conventional InP system.[1,2] By introducing a strain-compensated barrier to this system, it is possible to grow a highly strained InGaAsN well free of misfit dislocations to improve the carrier confinement and increase the numbers of QWs in the laser structure.[10–13] There have been several works investigating the growth of InGaAsN QWs with GaAsN as the direct barrier,[4,6,8,10,13,14] which, however, is a smaller band-gap material system than GaAs. The utilization of larger band-gap barrier materials will lead to a suppression of thermionic carrier leakage, which will, in turn, lead to a reduction in the temperature sensitivity of the threshold-current density of the lasers, in particular, at high-temperature operation.[15] The strain compensation of InGaAsN QW lasers using larger band-gap GaAsP tensile-strained barriers has been reported by Tansu *et al.*[7,9,12,16] and W. Li *et al.*[11]

In general, wafers for InGaAsN lasers are grown either by molecular beam epitaxy (MBE)[4,5] or by metal-organic chemical vapor deposition (MOCVD).[2,9,10] Very high output power operations have been demonstrated in InGaAsN broad-area lasers grown by both MBE (~4.2 W at a heatsink temperature of 10 °C and with facet coating)[3] and MOCVD (1.8 W at a heatsink temperature of 20 °C and with facet coating).[9] A very low threshold-current density (~210 A/cm^2) has been obtained in MOCVD broad-area single-quantum-well lasers.[7]

In this letter, we report on 100-μm stripe width ridge waveguide lasers grown by MOCVD and fabricated with pulsed anodic oxidation (PAO). Light output power reached 962 mW in cw mode at room temperature. The threshold current density was 256 A/cm^2.

In the fabrication of semiconductor lasers, a uniform and high-quality, current blocking layer is a critical component. This layer is usually formed by the deposition of oxides by plasma-enhanced chemical vapor deposition. This is costly and the fabrication process is relatively complicated. Pulsed anodic oxidation is a simple and cost-effective method for the fabrication of optoelectronic devices.[17] Previously pulsed anodic oxidation has been applied to QW intermixing in GaAs/AlGaAs and InGaAs/GaAs QW and quantum wire structures.[18] We have recently shown a significant reduction of threshold-current density in AlGaInP/GaInP lasers with pulsed anodic oxidation.[19]

The wafer used in this work was grown by MOCVD by IQE (Europe) Ltd. The active region consists of three $In_{0.35}Ga_{0.65}As_{0.985}N_{0.015}$ QWs (TQWs), each 6.4 nm thick, separated by 7-nm GaAs and 8-nm $GaAs_{0.82}P_{0.18}$ barriers. The active region is symmetrically embedded in a 35-nm-thick undoped GaAs waveguide. A 1.2-μm Si-doped (6×10^{17} cm^{-3}) *n*-type $Al_xGa_{1-x}As$ ($x=0-0.5$) cladding layer was grown between the *n*-substrate and active layer, and a 1.2-μm C-doped (5×10^{17} cm^{-3}) *p*-type $Al_xGa_{1-x}As$ ($x=0-0.5$) cladding layer followed the active layer. A 20-nm P^+ (1×10^{19} cm^{-3}) GaAs cap layer was grown for contacting. After wafer cleaning, 100-μm-wide photoresist stripes with a pitch of 300 μm were first made on the surface by standard photolithography, and the top contact GaAs and top cladding AlGaAs between the photoresist stripes were etched by standard selective wet etching (resulting in an etch depth of 1.23 μm). The oxide film was formed on the wafer by pulsed anodic oxidation. A vacuum tube was used as the vacuum tweezers to hold the sample and conduct current. The electrolyte was made of ethylene glycol: phosphoric acid: de-ionized water (40:20:1 by volume). The pulsed width was 1 ms, while the pulsed period was 12 ms. The total anodization time was 4 min. After anodization, samples were rinsed with de-ionized water, followed by a rinse with a resist stripper to remove the photoresist, then by de-ionized water, and was finally nitrogen blow dried.[20] The wafer was then thinned and contact metals were deposited by electron beam evaporation. The laser chips were *p*-side-down bonded onto copper heatsinks with indium. The details of the bonding were published elsewhere.[21] Figure 1 shows a scanning electronic microscope (SEM) image of the InGaAsN laser fabricated with pulsed anodic oxidation.

The lasers were tested without facet coating under cw operation. Output power (P) versus injection current (I) characterization of the laser was performed using a calibrated

[a]Author to whom correspondence should be addressed; electronic mail: yqu@ntu.edu.sg
[b]Electronic mail: shu.yuan@ieee.org

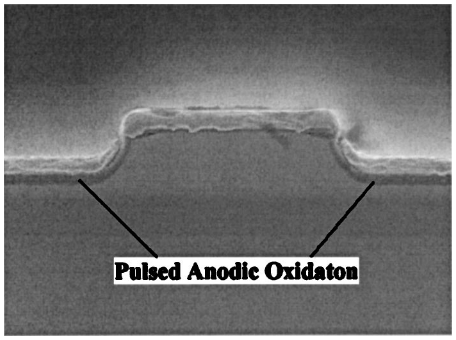

FIG. 1. SEM image of a ridge waveguide laser diode fabricated with pulsed anodic oxidation.

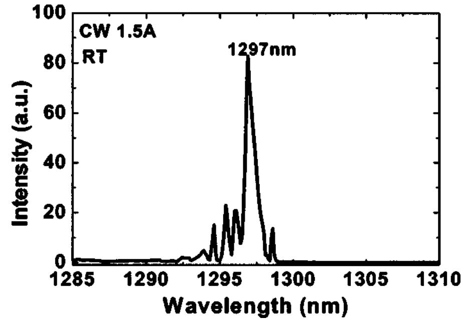

FIG. 3. A typical lasing spectrum of the laser in Fig. 2 at an injection current of 1500 mA.

InGaAs detector mounted on an integration sphere. The laser emission spectra were measured in a cw mode using a spectrometer, a Ge detector (cooled down to −20 °C), and a data acquisition system. A heatsink with a laser chip on it was then mounted on a standard TO-3 can. During the characterization of the laser, the cap of the TO-3 can was removed, and the laser was placed in front of the entrance of a Newport integration sphere.

The room-temperature P–I characteristics of a 100 μm $\times$ 1500 μm triple-QW-uncoated laser in cw mode is shown in Fig. 2. We stopped the measurement when the laser power reached 962 mW. The maximum slope efficiency was 0.42 W/A in the linear region. The threshold current was 385 mA, corresponding to a threshold-current density of 256 A/cm^2. Tansu *et al.*[10] recently reported the lowest threshold-current densities of 210–270 A/cm^2 for single-QW InGaAsN lasers with cavity lengths from 1000 to 2000 μm. Kovsh *et al.*[22] recently reported 1.3-μm ridge waveguide single-QW InGaAsN lasers with a differential quantum efficiency of 62%. Their lasers were antireflection/high-reflection facet coated, and bonded to heatsinks and packaged in to the TO-46 packages.

A plot of the relationship between the reciprocal of the external differential quantum efficiency η_d and the cavity length L yielded the internal quantum efficiency η_i and the internal loss α_i for unbonded 10-μm stripe lasers. The intercept gives η_i, and this can be used in the slope to get α_i. η_i and α_i were found to be 92% and 12 cm^{-1}, respectively, for this wafer. In contrast to the laser shown in Fig. 2, these uncoated lasers were not bonded by indium on the TO-3 package, but were placed on a homemade spring-loaded jig during testing.

The lasing spectrum of the 100 μm $\times$ 1500 μm triple-QW laser at room temperature in cw mode is shown in Fig. 3. The emission wavelength at 1500 mA was 1297 nm. The temperature-dependent laser powers versus current curves are shown in Fig. 4. The laser operated up to 100 °C. A plot of $\ln(I_{th})$ versus temperature was linear up to about 80 °C, and yielded a characteristic temperature of 138 K.

Conventional methods for the fabrication of ridge waveguide lasers usually require the deposition of SiO_2 or Si_3N_4 by the plasma-enhanced CVD method, which requires more processing steps, and thus increases the chance of process-induced damage (e.g., plasma damage). SiO_2 reacts easily with Al in the AlGaAs cladding layer, leaving behind Si atoms as impurities in the p-cladding layer, while both SiO_2 and Si_3N_4 cause considerable stress in the underlying layers due to lattice mismatch.[23] The stress increases interface defect densities. For laser fabrication with PAO, however, such problems are avoided. Since the oxides were native oxides formed at room temperature, it caused little damage to the device, and served as a passivation layer that reduced the interface trapping centers. In our work, higher photoluminescence intensity was observed from anodized samples than from as-grown samples.

In addition, heat dissipation is critical for laser operation, as the electrical power density in the ridge is very high (~5.6 kW/cm^2 for the laser in Fig. 2 at an operation current of 4.0 A). Anodic oxides are composed of various oxides of aluminum (its thermal conductivity is 25.08 W/m K), arsenic, and gallium, and have higher thermal conductivity than SiO_2 (its thermal conductivity is 1.4 W/m K). Thus, heat generated during the operation of the lasers is removed

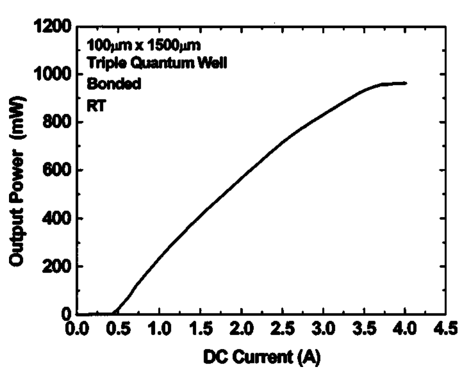

FIG. 2. Room-temperature cw light output power from a single facet vs injection current for a 100 μm $\times$ 1500 μm ridge waveguide InGaAsN laser diode fabricated with pulsed anodic oxidation. The laser was not facet coated, but was bonded p-side down on copper heatsinks with indium.

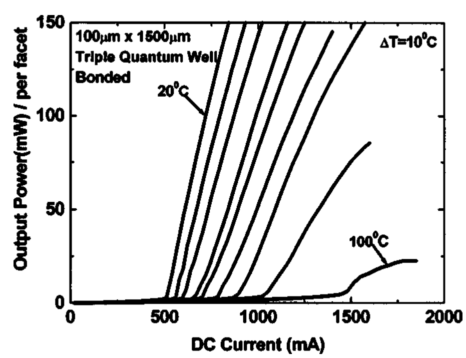

FIG. 4. Temperature-dependent optical power versus current characteristics of the InGaAsN triple-QW laser in Fig. 2. It lased up to 100 °C. The characteristic temperature was 138 K in the linear region (20–80 °C).

more efficiently in PAO lasers. Bonding of the ridge waveguide lasers to the heatsink using indium plays an important role in the operation of the lasers in this work. The contact between the laser and heatsink is also much more intimate with indium bonding.

It was well established[4,12] that strain-compensated layers can enhance device performance by allowing higher indium concentration (for longer wavelengths) and lower nitrogen concentration (for improving luminescence efficiency) to be used in the active region. The GaAsP layers used in this work were close to the InGaAsN layers and had a higher band gap than GaAs, and thus the carrier confinement was enhanced. The tensile strain in the GaAsP also reduced the overall stress of the active region (strain compensation). Therefore, stress-related defects were reduced in the active region. These effects may have a significant contribution to the overall satisfactory performance of the lasers.

The lasers in this work had three QWs, in contrast to the single well in Ref. 22. Lasers were fabricated using conventional methods (i.e., not by the PAO method) and using wafers grown under similar conditions but having different number of quantum wells; there was no conclusive direct correlation between slope efficiency and the number of quantum wells.[24] Thus it is unlikely that the wafer structure affected the laser performance significantly.

In conclusion, pulsed anodic oxidation was applied to the fabrication of ridge waveguide InGaAsN triple-QW strain-compensated lasers grown by MOCVD. Laser output power reached 962 mW in cw mode at room temperature from 100-μm stripe lasers. The lasing wavelength of a 100 $\mu m \times 1500$ μm triple-QW laser in cw mode at room temperature was 1297 nm. The threshold-current density was 256 A/cm^2. The maximum slope efficiency was found to be 0.42 W/A at room temperature. The characteristic temperature was 138 K (20–80 °C). The lasers operated up to 100 °C. Possible reasons for the reasonable device performance were discussed.

The authors would like to thank Li Xu, B. X. Bo, G. J. Liu, H. L. Jiang, and co-workers of the National Key Laboratory on High Power Semiconductor Lasers at the Changchun University of Science and Technology for help with the bonding devices. They also thank S. G. Ma, Dr. S. Z. Wang, and Dr. S. F. Yoon for helpful discussions.

[1] M. Kondow, T. Kitatani, S. Nakatsuka, M. C. Larson, K. Nakahara, Y. Yazawa, M. Okai, and K. Uomi, IEEE J. Sel. Top. Quantum Electron. **3**, 719 (1997).
[2] S. Sato and S. Satoh, IEEE Photonics Technol. Lett. **11**, 1560 (1999).
[3] D. A. Livshits, A. Yu, Egorov, and H. Riechert, Electron. Lett. **36**, 1381 (2000).
[4] W. Li, T. Jouhti, C. S. Peng, J. Konttinen, and P. Laukkanen, Appl. Phys. Lett. **79**, 3386 (2001).
[5] J. Wei, F. Xia, C. Li, and S. R. Forrest, IEEE Photonics Technol. Lett. **14**, 597 (2002).
[6] C. S. Peng, T. Jouhti, P. Laukkanen, E.-M. Pavelescu, J. Konttinen, W. Li, and M. Pessa, IEEE Photonics Technol. Lett. **14**, 275 (2002).
[7] N. Tansu, N. J. Kirsch, and L. J. Mawst, Appl. Phys. Lett. **81**, 2523 (2002).
[8] W. Ha, V. Gambin, M. Wistey, S. Bank, S. Kim, and J. S. Harris, Jr., IEEE Photonics Technol. Lett. **14**, 591 (2002).
[9] N. Tansu, A. Quandt, M. Kanskar, W. Mulhearn, and L. J. Mawst, Appl. Phys. Lett. **83**, 18 (2003).
[10] N. Tansu, J.-Y. Yeh, and L. J. Mawst, Appl. Phys. Lett. **83**, 2512 (2003).
[11] W. Li, J. Turpeinen, P. Manen, P. Savolainen, P. Uusimaa, and M. Pessa, Appl. Phys. Lett. **78**, 91 (2001).
[12] N. Tansu and L. J. Mawst, IEEE Photonics Technol. Lett. **14**, 444 (2002).
[13] T. Jouhti, C. S. Peng, E.-M. Pavelescu, J. Konttinen, L. A. Gomes, O. G. Okhotnikov, and M. Pessa, IEEE J. Sel. Top. Quantum Electron. **8**, 787 (2002).
[14] S. G. Spruytte, M. C. Larson, W. Wampler, C. W. Coldren, H. E. Petersen, and J. S. Harris, J. Cryst. Growth **227-228**, 506 (2001).
[15] K. Nakahara, M. Kondow, T. Kitatani, M. C. Larson, and K. Uomi, IEEE Photonics Technol. Lett. **10**, 487 (1998).
[16] N. Tansu, J.-Y. Yeh, and L. J. Mawst, Appl. Phys. Lett. **82**, 3008 (2003).
[17] M. J. Grove, D. A. Hudson, P. S. Zory, R. J. Dalby, C. M. Harding, and A. Rosenberg, J. Appl. Phys. **76**, 587 (1994).
[18] S. Yuan, Y. Kim, C. Jagadish, P. T. Burke, M. Gal, J. Zhou, D. Q. Cai, D. J. H. Cockayne, and R. M. Cohen, Appl. Phys. Lett. **70**, 1269 (1997).
[19] C. Y. Liu, Shu Yuan, J. R. Dong, S. J. Chua, M. C. Y. Chan, and S. Z. Wang, J. Appl. Phys. **94**, 2962 (2003).
[20] S. Yuan, C. Jagadish, Y. Kim, Y. Chang, H. H. Tan, R. M. Cohen, M. Petravic, L. V. Dao, M. Gal, M. C. Y. Chan, E. H. Li, O. Jeong-seok, and P. S. Zory, IEEE J. Sel. Top. Quantum Electron. **4**, 629 (1998).
[21] Yi Qu, S. Yuan, C. Y. Liu, B. X. Bo, G. J. Liu, and H. L. Jiang, IEEE Photonics Technol. Lett. **16**, 389 (2004).
[22] A. R. Kovsh, J. S. Wang, R. S. Hsiao, L. P. Chen, D. A. Livshits, G. Lin, V. M. Ustinov, and J. Y. Chi, Electron. Lett. **39**, 1726 (2003).
[23] S. Yuan, Y. Kim, C. Jagadish, P. T. Burke, M. Gal, M. C. Y. Chan, E. H. Li, and R. M. Cohen, J. Appl. Phys. **83**, 1305 (1998).
[24] Broad-area (50-μm-wide contact stripe) InGaAsN lasers with single, double, and triple QWs were fabricated from wafers grown by IQE Europe Ltd. No current blocking layer was used. For 1200-μm-long lasers, the slope efficiency was 0.096, 0.050, and 0.118 W/A, respectively, private communication.